Bioorganic Chemistry 88 (2019) 102968

Contents lists available at ScienceDirect

Bioorganic Chemistry

journal homepage: www.elsevier.com/locate/bioorg

Synthesis and evaluation of Quinoline-3-carbonitrile derivatives as potential antibacterial agents

Salman A. Khan[a,*], Abdullah M. Asiri[a,b], Hadi Mussa Basisi[a], Mohammad Asad[a], Mohie E.M. Zayed[a], Kamlesh Sharma[c], Mohmmad Younus Wani[d,*]

[a] Chemistry Department, Faculty of Science, King Abdulaziz University, P.O. Box 80203, Jeddah 21589, Saudi Arabia
[b] Center of Excellence for Advanced Materials Research (CEAMR), King Abdulaziz University, P.O. Box 80203, Jeddah 21589, Saudi Arabia
[c] Department of Chemistry, Faculty of Sciences, Shree Guru Gobind Singh Tricentenary University, Gurugram 122505, Haryana, India
[d] Chemistry Department, Faculty of Science, University of Jeddah, P.O. Box 80327, Jeddah 21589, Saudi Arabia

ARTICLE INFO

Keywords:
Quinoline-3-carbonitrile
DFT (Density Function Theory)
Antibacterial
Physicochemical properties
Docking

ABSTRACT

New quinoline-3-carbonitrile derivatives were synthesized and evaluated for their potential antibacterial behavior. Compounds were obtained by a one-pot multicomponent reaction of appropriate aldehyde, ethyl cyanoacetate, 6-methoxy-1,2,3,4-tetrahydro-naphthalin-1-one and ammonium acetate. Structures were established by different physical and spectroscopic techniques. The molecular geometry, vibration frequencies, HOMO–LUMO energy gap, molecular hardness (g), ionization energy (IE), electron affinity (EA), and total energy of these compounds was assessed by DFT studies, employing DFT/RB3LYP method. Preliminary antibacterial studies using both Gram-positive and Gram-negative bacterial strains and cytotoxicity studies on mammalian cells revealed their promising antibacterial activity, without causing any severe host toxicity. All the compounds (QD1-QD5) in this study obeyed the 'Lipinski's Rule of Five' with logP values < 5 and HBA < 10, hydrogen bond donor's < 5. The most active compound **QD4** showed good interaction with the target DNA gyrase; target enzyme for quinoline class of antibiotics, which reveals its probable mechanism of action. Results of all these studies establish these compounds as important scaffolds with broad-spectrum antibacterial activity with no off-target toxicity. Having lower band gap energy of 3.40 eV and a low lying LUMO for compound **QD4,** this compound may be a valuable starting point for the development of quinoline-3-carbonitrile based broad-spectrum antibacterial agents.

1. Introduction

The quinoline ring system is an important structural unit in naturally occurring quinoline alkaloids, therapeutics, synthetic analogues with interesting biological activities, and many standard drugs as well [1]. In fact, introducing chloroquine into treatment of malaria more than 60 years ago triggered a new era of quickly developing antimicrobial drugs. In synthetic medicinal chemistry the quinoline motif is widely exploited, revealing a spectrum of activity covering antimalarial, anticancer, antifungal, antibacterial, antiprotozoic, antibiotic, and anti-HIV [2–8]. The synthetic antibacterial agents that include cinoxacin, ciprofloxacin, nalidixic acid, norfloxacin, and ofloxacin belong to the quinolone class of compounds, sharing quinoline as the basic ring skeleton (Fig. 1). The quinolone class of antibacterials has been spectacularly successful and continues to dominate the field of antibacterial therapeutics with great influence [9]. Quinolone antibiotics target DNA gyrase, a type II topoisomerase, catalysing the seemingly complex reaction of DNA supercoiling by interrupting the DNA breakage-reunion cycle of gyrase [10–13]. Therefore, development of quinolone based compounds, as antibacterial agents will add to the repertoire of antibiotics to combat drug resistance [14].

The success of a new compound to emerge as a lead molecule also strongly depends on its physicochemical properties [15–23]. Poor physicochemical properties of a biologically potent molecule obturate its use as a drug. Therefore evaluation of these properties is immensely important before a molecule undergoes *in vivo* and clinical studies [16,18,21]. The antimicrobial properties of biologically active molecules have also been ascribed to different electronic parameters of a molecule. It is believed that the antimicrobial property of compounds is a function of LUMO (Lowest Unoccupied Molecular Orbital) energy. LUMO is an electronic parameter, which measures the electrophilicity of the molecules. When a molecule acts as a Lewis acid, incoming

* Corresponding authors.
E-mail addresses: sahmad_phd@Yahoo.co.in (S.A. Khan), mwani@uj.edu.sa (M.Y. Wani).

https://doi.org/10.1016/j.bioorg.2019.102968
Received 2 January 2019; Received in revised form 26 March 2019; Accepted 29 April 2019
Available online 30 April 2019
0045-2068/

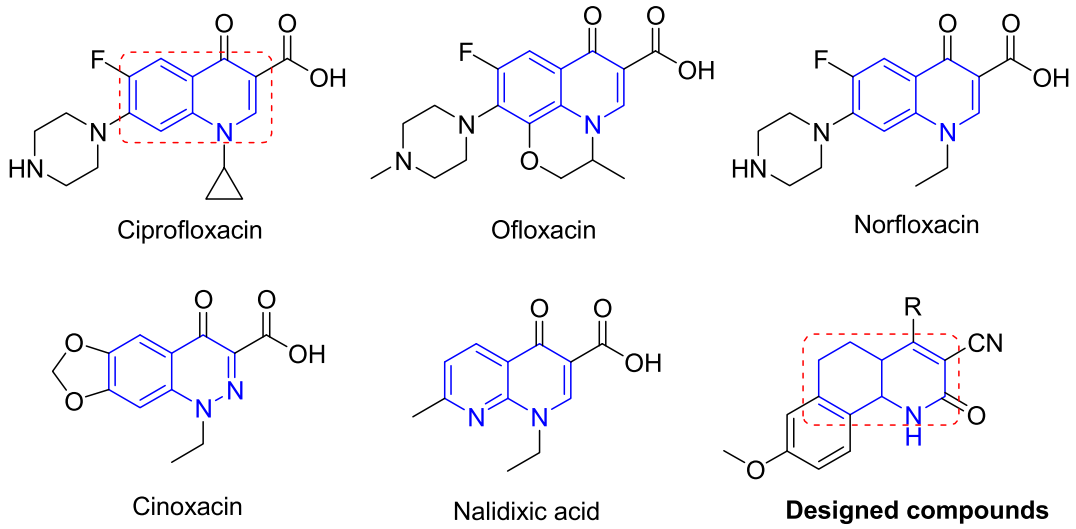

Fig. 1. Structures of the standard quinoline antibiotics and the designed compounds.

electrons are received in its LUMO. Molecules with low-lying LUMO are more able to accept electrons than those with high energy LUMO, and hence show higher activity [24,25].

Based on these facts and in view of the pressing demand for the search of new treatment strategies which could help better target bacteria and augment the current treatment options, we designed a series of quinoline derivatives and evaluated their physicochemical and biological behavior. We applied *ab initio* molecular computing using the density functional theory (DFT) calculations to gain insight into the electronic structure of the molecules to fully understand the experimental data. Docking studies were performed to establish their probable mechanism of action by inhibiting DNA gyrase; an important target of the quinolone class of antibiotics.

2. Results and discussion

2.1. Chemistry

The synthesis of Quinoline-3-carbonitrile derivatives **(QD1-QD5)** was achieved by a one-pot multicomponent reaction (MCR) of 6-methoxy-1,2,3,4-tetrahydro-naphthalin-1-one, the appropriate aldehydes, an excess of ammonium acetate and ethyl cyanoacetate as shown in Scheme 1. The purified products were characterized by the FT-IR, ^{1}H NMR, ^{13}C NMR and MS (ESI^{+}) spectra. The IR spectrum of compounds shows a characteristic band at 3233–3258 cm^{-1} due to presence of −NH group and at 1600–1638 cm^{-1} attributed to the C=O group. IR spectra also shows a C=N stretch at 1234–1288 cm^{-1}, which conforms the formation of quinoline derivatives (**QD1-QD5**). The ^{1}H NMR spectra of all the compounds measured at room temperature shows one singlet at 8.71–8.11 ppm for the NH. The appearance of different peaks in the range δ 8.02–6.47 are due to aromatic protons which have been assigned as singlets (s), doublets (d) or double doublets (dd) to their respective protons in the experimental section. Two multiplets at δ 2.76–2.54 and 2.56–2.34 ppm correspond to the benzylic protons (C6-*H* and C5-*H* respectively) (see experimental Section 3.3). Moreover, ^{13}C NMR spectra showed signals in the range of δ 156.48–120.00 ppm and at δ 1169.28–165.56 ppm due to aryl carbon and pyridine carbon, respectively. Characteristic molecular ion and fragmentation peaks were observed in the mass spectra of all the compounds (**QD1-QD5**). The mass spectrum of compound **QD1** shows a molecular ion peak ($M^{+\cdot}$) *m/z* 421. All the compounds followed a similar fragmentation pattern.

2.2. Physicochemical properties

The importance of physicochemical properties in designing bioavailable drugs has been widely recognized and increased efforts have been spent on assessing the drug "developability" based on calculated and measured physicochemical parameters [15–19]. The pKa,

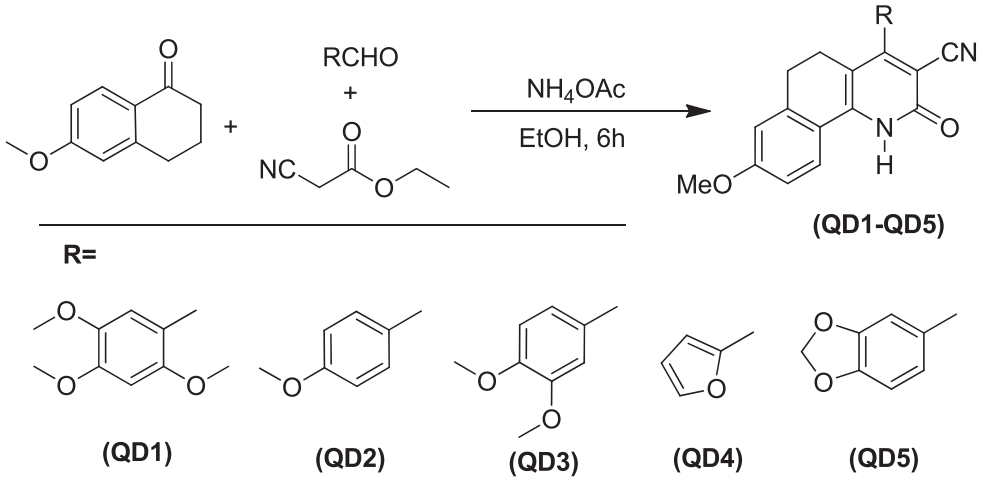

Scheme 1. Synthesis of Quinoline 3-carbonitrile derivatives (QD1-QD5).

solubility, and lipophilicity are among the most fundamental physicochemical properties of a drug candidate, and their measurements are essential for both *in silico* and *in vitro* evaluation of drug-like properties [15–23]. They are also the fundamental parameters for assessing ADMET (absorption, distribution, metabolism, excretion and toxicity) properties of drug candidates, whose deficiencies account for 50–60% of compound failures during development [22]. The optimal range of lipophilicity for good drug candidates lies in a narrow range of logD between ~1 and 3 [19] or ≤5 (Lipinski's Ro5) [20], and to achieve a solubility of > 100 μM, a typical desirable value for drug molecules [21], it requires a logP value < 3.25. In general, a lower log P means increased compound solubility [22,23]. Good intestinal absorption, reduced molecular flexibility (measured by the number of rotatable bonds), low polar surface area (PSA) or total hydrogen bond count (sum of donors, HBDs and acceptors, HBAs), are also important predictors of good oral bioavailability. Molecular properties such as membrane permeability and bioavailability are associated with logP, molecular weight (MW), or hydrogen bond acceptors and donors count in a molecule. The rule states that most molecules with good membrane permeability have logP < 5, molecular weight < 500, number of hydrogen bond acceptors < 10, and number of hydrogen bond donors < 5. This rule is widely used as a filter for drug-like properties. All the compounds (QD1-QD5) in this study obeyed the 'Rule of Five' with logP values < 5 and HBA < 10, hydrogen bond donor's < 5 as shown in Table 1. The most active compound **QD4** has properties more closer to the standard drugs compared to the other derivatives. Therefore this compound could be put to further advanced studies to unravel its potential.

2.3. DFT studies

2.3.1. Frontier molecular orbital analysis

The frontier orbitals (HOMO and LUMO) of chemical species are very important in defining their reactivity [26]. Higher value of HOMO of a molecule has a tendency to donate electrons to appropriate acceptor molecule with low energy empty molecular orbitals. The total energy, highest occupied molecular orbital (HOMO) energy, the lowest unoccupied molecular orbital (LUMO) energy, hardness (η), ionization energy (IE), electron affinity (EA) have been calculated and summarised in Table 2. DFT calculations showed that the molecule **QD4** has 3.40 eV energy gap which is lower than all other studied molecules (QD**1**, **QD2**, **QD3** and **QD5)**. These results indicate that the molecule **QD4** is comparatively softer than rest of the molecules as shown in Fig. 2. Our theoretical results correlate well with obtained experimental results. As well, the molecule with higher energy gap (E_{gap} = 3.59 eV) has shown poor antibacterial activities. Further, these results are supported by the literature as is reported that an electronic system with a larger HOMO-LUMO gap should be less reactive than the one having smaller gap. The decrease in the HOMO and LUMO energy gap explains the eventual charge transfer interaction taking place within the molecule due to the strong electron-accepting ability of the electron acceptor group. The strong charge transfer interaction is responsible for the bioactivity of the molecule [27].

The ionization energy (IE) can be expressed through HOMO orbital energies as IE = $-\varepsilon_{HOMO}$ and electron affinity (EA) can be expressed through LUMO orbital energies as EA = $-\varepsilon_{LUMO}$. The hardness (η) corresponds to the energy gap between HOMO and LUMO orbital. Larger the HOMO–LUMO orbital energy gap, harder the molecule. The hardness is also associated with the stability of the chemical system as shown in Fig. 3. Hardness and stability are directly proportional to each other. The theoretical calculations are performed in gaseous phase and the experimental results of molecules were recorded in solid or liquid phase. In spite of the differences, calculated physicochemical properties and frontier orbitals represent a good approximation of antibacterial activities of the molecules.

Table 1
Lipinski's tools for measuring drug likeness.

Compound	M.W	LogP	LogD*	No. of HBAs[a]	No. of HBDs[a]	PSA
QD1	416.43	2.91	1.72	6	1	89.81
QD2	356.37	3.17	2.04	4	1	71.35
QD3	386.13	3.04	1.88	5	1	80.58
QD4	316.08	1.91	1.23	3	1	71.35
QD5	370.10	3.07	1.82	5	1	80.58
Ciprofloxacin	331.34	1.32	−1.13[#]	6	2	72.88
Levofloxacin	361.14	1.35	NA	7	1	73.32

* At pH 7.4.
[a] HBA—hydrogen bond acceptor, HBD—hydrogen bond donor, PSA—polar surface area obtained by Marvin Sketch 5.1.
[#] Values adopted from referred sources. NA: Data not available.

2.4. Molecular docking studies

Molecular docking study of the newly synthesized compound **QD1-QD4** was performed to gain insights into its probable mechanism of action. 2D structure of the synthesized ligand molecules was converted to energy minimized 3D structure and was further used for docking. Bacterial DNA gyrase was taken as the target receptor and the binding pocket was validated by performing redocking of the ligand (clorobiocin). The binding pocket and the interaction of the ligand in complex with DNA gyrase is shown in Fig. 4. Molecular docking calculations of all the test compounds were carried out with Auto dock vina [28]. The conformation with the lowest binding free energy was used for analysis. All molecular docked models were prepared using PyMOL viewer. Docked images of the most active compound (**QD4**) are shown in Fig. 5. Binding energy and other parameters of all the docked compounds including the standard drugs is presented in Table 3. The docking studies revealed that the synthesized molecule **QD4** has less binding energy towards the target and several molecular interactions were responsible for the observed affinity. The best docking energy model and most possible interaction mode of the most active compound (**QD4**) and 1KZN is shown in Fig. 4. It was observed that the compound mainly interacts with the target enzyme by showing hydrogen bonding interaction with GLU50, ASP73, and GLY77 residues, mimicking clorobiocin that shows interaction with ASN46, ASP73, ARG136 aminoacid residues (see Fig. 4). Besides hydrophobic and Van der Waals interactions were also involved. Binding affinity value of the docked target compounds were found to be in the range −8.6 to −10.8 kcal mol^{-1}. The results revealed that the quinoline ring NH and C═O show strong hydrogen bonding interaction with the amino acid residues of the protein, which clearly advocates its better antibacterial efficacy. The presence of a furan ring in **DQ4** in place of other substituted phenyl rings in other derivatives may have helped this compound to obtain optimum electron density and proper orientation to fit in the active site of the enzyme. From these results it can be inferred that compound **QD4** probably shows its antibacterial activity in a similar way as that of the quinoline antibiotics by interfering with the functioning of DNA gyrase. The structure of the quinoline-3 carbonitrile derivative **DQ4** can be further optimized by using different heteroaromatic rings in place of the furan ring for more detailed structure-activity relationship studies.

2.5. Antimicrobial activity

2.5.1. Disc diffusion assay

The compounds **(QD1-QD5)** were tested for their antibacterial activities by disc-diffusion method using nutrient broth medium. Two Gram-positive bacteria and two Gram-negative bacteria utilized in this study consisted of *Staphylococcus aureus, Streptococcus pyogenes*, *Escherichia coli* and *Salmonella typhimurium*. All the test compounds showed varying range of antibacterial activities against the selected panel of pathogens, as is evident from the zone of inhibitions (ZOI),

Table 2
Physicochemical data of compounds **QD1-QD5** calculated by using DFT/RB3LYP/6-31G*

Compound	Total Energy (kcal/mol)	HOMO (eV)	LUMO (eV)	Energy gap (eV)	Hardness[a] (η)	IE = $-\varepsilon_{HOMO}$	EA = $-\varepsilon_{LUMO}$
QD1	−886907.638	−5.52	−1.94	3.59	1.79	5.52	1.94
QD2	−743186.810	−5.63	−2.07	3.56	1.78	5.63	2.07
QD3	−815043.379	−5.64	−2.06	3.58	1.785	5.64	2.06
QD4	−669923.402	−5.74	−2.34	3.40	1.7	5.74	2.34
QD5	−789623.987	−5.66	−2.18	3.48	1.74	5.66	2.18

[a] Hardness (ç) = ½ (HOMO - LUMO).

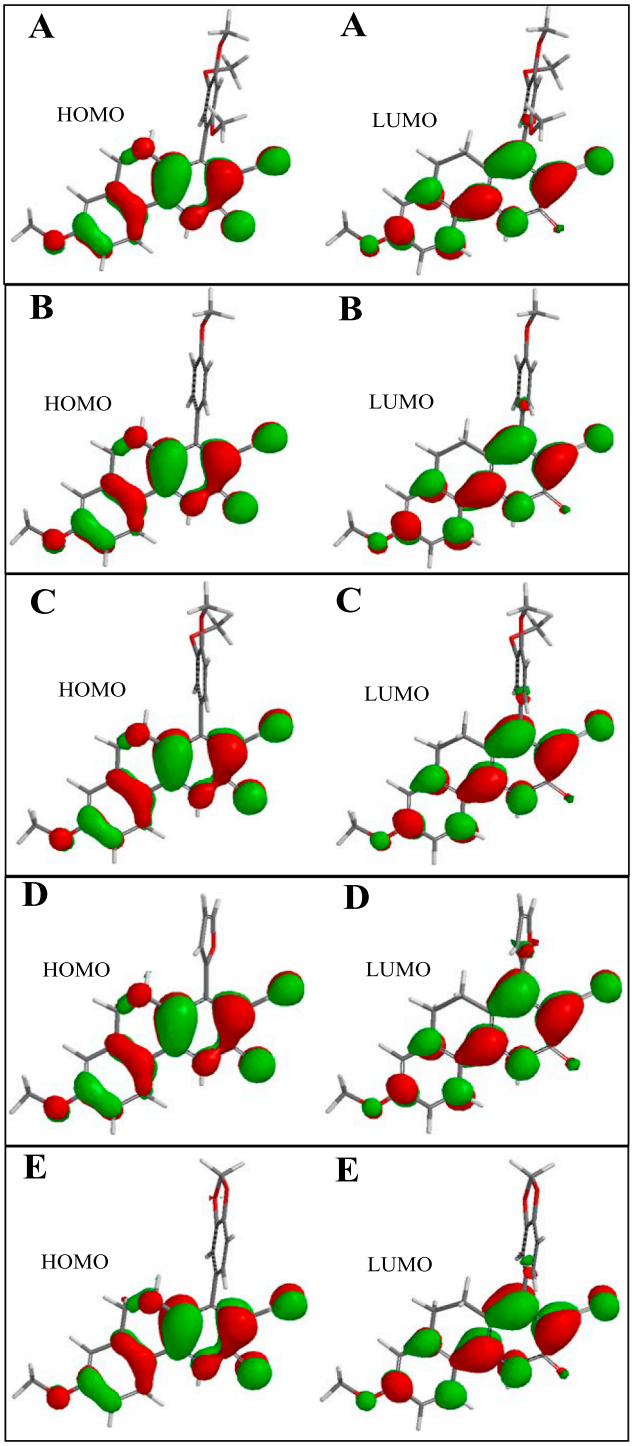

Fig. 2. Highly occupied and lowest unoccupied molecular orbitals of compounds **QD1-QD5** represented as A-E.

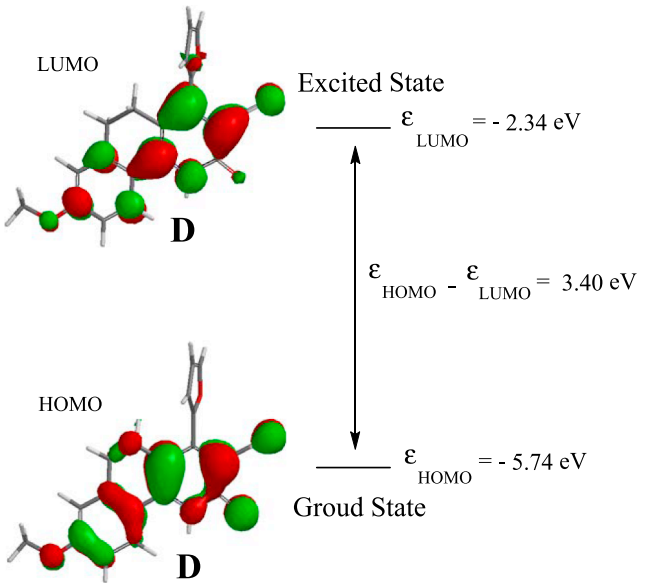

Fig. 3. Molecular orbital surface and HOMO-LUMO energy gap for compound **QD4** obtained by density functional theory.

presented in Table 4. The results showed that among the five compounds tested, furan substituted qunioline derivative **QD4** showed comparatively higher antibacterial activity than the other derivatives.

2.5.2. Minimum Inhibitory Concentrations (MIC)

Evaluation of the MIC values by broth dilution assay, showed that all the test compounds were active *in vitro* against both Gram-positive as well as Gram-negative bacteria (Table 5). The furan substituted qunioline derivative **(QD4)**, exhibited high antibacterial activity with MIC ranging from 4 to 8 μg/mL against all strains of bacteria tested. The MIC values of other compounds are 2–3 fold higher than the most active compound. Ciprofloxacin as a positive control showed MIC in the range of < 1–2 μg/mL against the tested strains as shown in Table 5.

2.6. In vitro cytotoxicity studies

3-(4,5-Dimethylthiazol-2-yl)-2,5-diphenyl tetrazolium bromide (MTT) is reduced by the succinate dehydrogenase system of mitochondrial living cells to produce water insoluble purple formazan crystals which, after solubilization can be measured spectro-photometrically [29]. Since the amount of formazan produced is directly proportional to the number of active cells in the culture, MTT has long been used to assess the cell viability in cell proliferation and cytotoxicity [29,30].

Compounds **QD1-QD5** were screened for their antibacterial activity and then evaluated for their cytotoxicity against MDA-MB-231 cell line to ensure any cytotoxicity to the mammalian host. A sub-confluent population of MDA-MB-231 cells was treated with increasing concentration of these compounds and the number of viable cells was measured after 48 h by MTT cell viability assay. The concentration

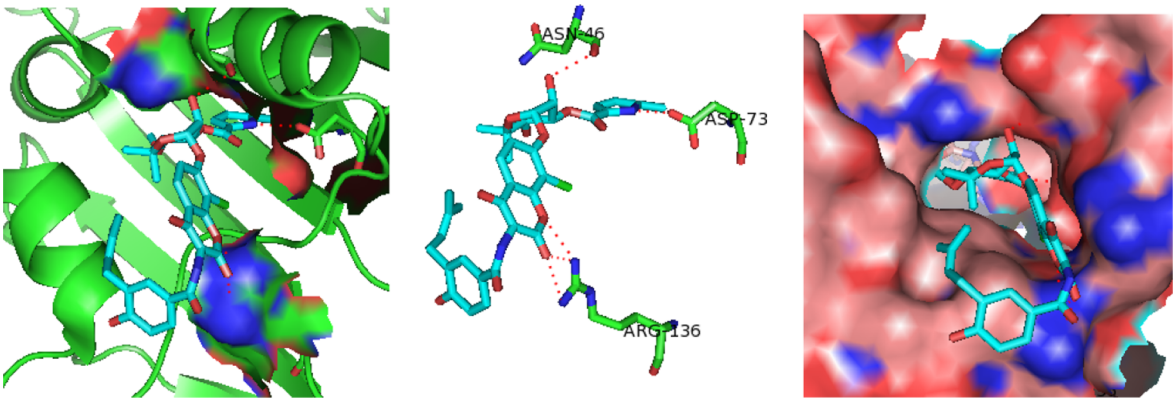

Fig. 4. Crystal structure and binding pocket of the ligand (clorobiocin) in complex with DNA gyrase and interaction of the ligand with different aminoacid residues in the pocket.

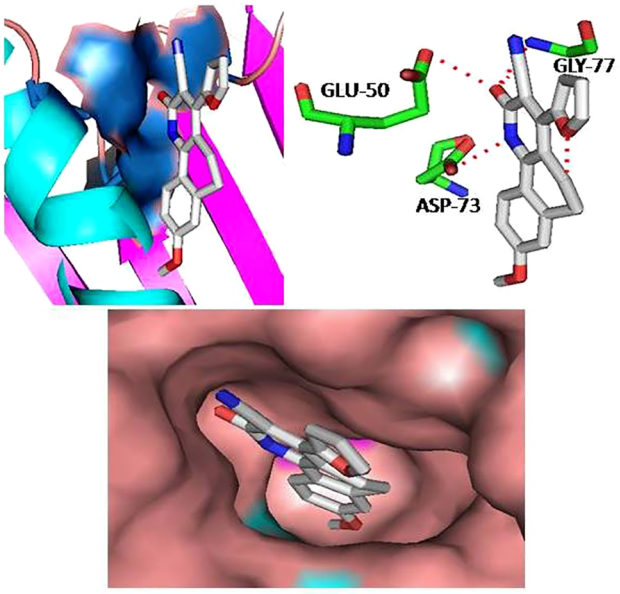

Fig. 5. Docking poses of the most active compound (**QD4**) with DNA gyrase 1KZN.

Table 3
Binding affinity values and other parameters of the docked compound DQ4.

Compound	Binding affinity values (kcal/mol)	Amino acid residues	H-bond
QD1	−8.6	ASP-49, PRO-75	2
QD2	−10.2	ALA47, ARG76	2
QD3	−8.9	GLY-81	1
QD4	−10.8	GLU-50, ASP-73, GLY-77	3
QD5	−10.6	GLN72	1

range of all the compounds was 3.13–100 µM. The cell viability (%) obtained with continuous exposure for 48 h are depicted in Fig. 6. The cytotoxicity of all the compounds was found to be concentration-dependent. Fig. 6 depicts that all the test compounds showed 100% viability, at concentration of 3.13 µM and up to a concentration of 25 µM all the compounds showed a viability of ≥70%. On increasing the concentration range from 50 to 100 µM the percentage viability began to decrease which indicates the increase in toxicity of the test compounds. Compound QD**2** is comparatively more cytotoxic than QD**1** and QD**3**, whereas compound QD**4** and QD**5** are the least cytotoxic with IC_{50} values higher than 100 µM. From these results it can be inferred

Table 4
Antibacterial activity in terms of ZOI (mm) of compounds **QD1-QD5**.

Compounds	Zone of Inhibition ZOI (mm) 10 µg mL^{-1}/disc			
	S. aureus	*S. pyogenes*	*S. typhimurium*	*E. coli*
QD1	12.4 ± 0.4	11.2 ± 0.5	11.8 ± 0.5	14.2 ± 0.5
QD2	12.6 ± 0.3	12.8 ± 0.3	10.6 ± 0.2	10.5 ± 0.5
QD3	13.4 ± 0.5	14.2 ± 0.4	12.5 ± 0.4	16.5 ± 0.5
QD4	20.0 ± 0.3	22.8 ± 0.5	22.2 ± 0.4	24.5 ± 0.5
QD5	18.0 ± 0.4	16.5 ± 0.3	18.6 ± 0.4	18.8 ± 0.5
+Ve control	24.0 ± 0.5	22.2 ± 0.4	24.2 ± 0.8	26.0 ± 0.2
−Ve control	–	–	–	–

+Ve control: Ciprofloxacin; -Ve control: 1% DMSO measured by the Halo Zone Test (Unit, mm).

Table 5
Minimum inhibition concentration (MIC) of compounds QD**1-QD5**.

Bacterial strain	MIC (µg mL^{-1})					
	QD1	QD2	QD3	QD4	QD5	CIPRO#
S. aureus ATCC 29,213	32	32	32	8	32	< 1
S. pyogenes ATCC 19,615	64	32	32	4	16	2
S. typhimurium ATCC14028	64	16	16	4	32	< 1
E. coli ATCC 25,922	32	16	16	4	16	< 1

CIPRO#: Ciprofloxacin was used as a positive control

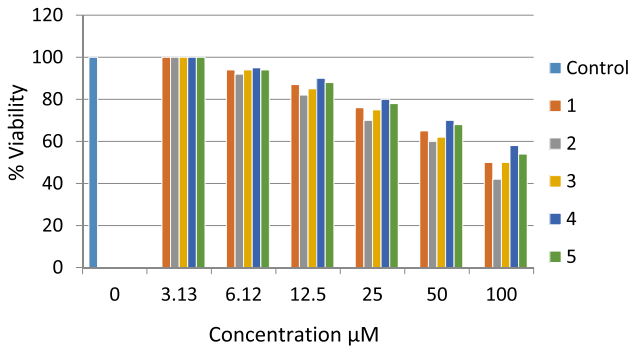

Fig. 6. Percentage viability of MDA-MB-231 cells after 48 h treatment with increasing concentration of compounds **QD1-QD5** represented as **1–5** respectively.

that **QD1-QD5** show good antibacterial activity and are non-cytotoxic to the mammalian cells.

Whlist the success of quinolone class of antibiotics is undeniable, they are no more considered as the blatant weapons against bacterial

infections. They are no more effective against many bacteria because of the development of drug resistance. Recently, the WHO published a list of bacteria for which new antibiotics are urgently needed [31], pressing the need to the development of new antibiotics or treatment strategies. It is estimated that 5–20 novel antibacterial drugs need to enter clinical development in order to effectively contend with the current resistance problem. The quinolones were the last broad spectrum antibiotics to enter the clinic and since then the discovery of novel, broad and narrow spectrum antibiotics has become difficult [32]. Although different antibiotic discovery programmes are currently underway, development of structural mimetic or derivatives of already established drugs is considered a good, albeit short-term strategy to tackle the growing antibiotic resistance problem and augment the current treatment options. Several new derivatives of the fluoroquinolone nucleus have already resulted in the development of third generation of drugs, moxifloxacin and gatifloxacin, both especially active against those bacteria resistant to beta-lactams. Subsequent development of fluoroquinolones has resulted in trovafloxacin and the prodrug alatrofloxacin and it is expected that further fluoroquinolones will be developed in the future, with a specific market in ocular infections and prophylaxis. In this study, we developed new quinoline based antibacterials and found a new lead molecule with interesting broad spectrum antibacterial activity, desirable physico-chemical properties, electronic parameters and interaction with the target DNA gyrase; target enzyme for quinoline class of antibiotics. This lead molecule could be further evaluated for its antibiotic potential by performing advanced studies.

3. Experimental

3.1. Materials

The appropriate aldehyde, 6-methoxy-1,2,3,4-tetrahydro-naphthalin-1-one, ethyl cyanoacetate and ammonium acetate were purchased from Acros Organic. Other reagents and solvents (A.R.) were obtained commercially and used without further purification.

3.2. General considerations

Melting points were recorded on a Thomas Hoover capillary melting apparatus without correction. FT-IR spectra were recorded on a Nicolet Magna 520 FT-IR spectrometer. ^{1}H NMR and ^{13}C NMR experiments were performed in $CDCl_3$ on a Brucker DPX 600 MHz spectrometer using tetramethyl silane (TMS) as internal standard at room temperature.

3.3. Synthesis of Quinoline-3-carbonitrile derivatives

Quinoline-3-carbonitrile derivatives (QD1-QD5) were obtained by a one-pot reaction of appropriate aldehydes (1 mmol), 6-methoxy-1,2,3,4-tetrahydro-naphthalin-1-one **1** (1 mmol), ethyl cyanoacetate (1.1 mmol) and ammonium acetate (2 mmol) in absolute ethanol under reflux for 6 h. The reaction mixture was allowed to cool and left overnight to precipitate. The precipitate was filtered, washed with water, collected, dried and recrystallized in methanol/dichloromethane [33].

3.3.1. 3-(2,4,5-trimethoxyphenyl)-8-methoxy-2-oxo-1,2,5,6 tetrahydrobenzo[h]quinoline-3-carbonitrile (QD1)

Yield: 73.08 (%); M.P: 160 °C; FTIR (KBr) ν_{max} cm^{-1}: 3258 (NH), 2938 (C−H), 2212 (CN), 1615 (C═O), 1568 (C═C), 1252 (N═C); ^{1}H NMR (600 MHz $CDCl_3$) (δ/ppm): 8.71 (s, NH), 8.02 (s, CHAr, 1H), 7.26 (s, CHAr, 1H), 6.87 (d, CHAr, 1H, J = 8.4 Hz), 6.68 (d, CHAr, 1H, J = 7.8 Hz), 6.47 (s, CHAr, 1H), 3.98 (s, 3H, OCH_3), 3.96 (s, 3H, OCH_3), 3.91 (s, 3H, OCH_3), 3.88 (s, 3H, OCH_3), 2.56–2.54 (m, 2H, CH_2cyclo, H-6, 2H), 2.36–2.34 (m, 2H, CH_2cyclo, H-5, 2H); ^{13}C NMR ($CDCl_3$) δ: 169.28 (pyridine C), 163.70 (C═O), 156.48, 155.41, 150.33, 148.37 (Ar-C), 117.21 (CN), 28.14 (C-5), 28.52 (C-6); Anal. calc. for $C_{24}H_{22}N_2O_5$: C, 68.89, H, 5.30, N, 6.69. Found: C, 68.82, H, 5.30, N, 6.65; ESI-MS m/z (rel. int. %): 421 (75) $[M+H]^+$

3.3.2. 8-methoxy-4-(4-methoxyphenyl)-2-oxo-1,2,5,6-tetrahydrobenzo[h] quinoline-3-carbonitrile (QD2)

Yield: 65.25 (%); M.P: 201 °C; FTIR (KBr) ν_{max} cm^{-1}: 3245 (NH), 2935 (C−H), 2217 (CN), 1600 (C═O), 1542 (C═C), 1288 (N═C); ^{1}H NMR (600 MHz $CDCl_3$) (δ/ppm): 8.56 (s, NH), 7.31–6.78 (m, 7H, CHAr) 3.89 (s, 3H, OCH_3), 3.86 (s, 3H, OCH_3), 2.76–2.73 (m, 2H, CH_2cyclo, C6), 2.53–2.51 (m, 2H, CH_2cyclo, C5); ^{13}C NMR ($CDCl_3$) δ: 166.53 (pyridine C), 163.17 (C═O), 154.45, 145.10, 141.47, 133.68, 130.18, 129.58, 127.40, 126.58, 127.40, 120.00 (Ar-C), 116.26 (CN), 114.79, 114.52, 113.77, 112.75, 62.42, 55.65, 55.51, 28.68 (C-5), 23.91 (C-6); Anal. calc. for $C_{22}H_{18}N_2O_3$: C, 73.73, H, 5.06, N, 7.82. Found: C, 73.68, H, 5.02, N, 7.81; ESI-MS m/z (rel. int. %): 360 (78) $[M+H]^+$

3.3.3. 4-(3,4-dimethoxyphenyl)-8-methoxy-2-oxo-1,2,5,6-tetrahydrobenzo[h]quinoline-3-carbonitrile (QD3)

Yield: 80.25 (%); M.P: 262 °C; FTIR (KBr)ν_{max} cm^{-1}: 3256 (NH), 2939 (C−H), 2220 (CN), 1629 (C═O), 1549 (C═C), 1272 (N═C); ^{1}H NMR (600 MHz $CDCl_3$) (δ/ppm): 8.16 (s, NH), 7.81–6.72 (m, 5H, CHAr) 3.91 (s, 3H, OCH_3), 3.83 (s, 3H, OCH_3), 3.72 (s, 3H, OCH_3), 2.75–2.71 (m, 2H, CH_2cyclo, C6), 2.52–2.49 (m, 2H, CH_2cyclo, C5); ^{13}C NMR ($CDCl_3$) δ: 167.58 (pyridine C), 163.15 (C═O), 153.69, 149.31, 127.92, 124.64, 120.98 (Ar-C), 118.76 (CN), 116.40, 111.95, 110.95, 99.43, 62.49, 56.09, 29.28 (C-5), 28.58 (C-6); Anal. calc. for $C_{23}H_{20}N_2O_4$: C, 71.12, H, 5.19, N, 7.21; Found: C, 71.07, H, 5.11, N, 7.17. ESI-MS m/z (rel. int. %): 391 (56) $[M+H]^+$

3.3.4. 4-(furan-2-yl)-8-methoxy-2-oxo-1,2,5,6-tetrahydrobenzo[h] quinoline-3-carbonitrile (QD4)

Yield: 75.45 (%); M.P: 169 °C; FTIR (KBr) ν_{max} cm^{-1}: 3238 (NH), 2948 (C−H), 2253 (CN), 1638 (C═O), 1565 (C═C), 1247 (N═C); ^{1}H NMR (600 MHz $CDCl_3$) (δ/ppm): 8.21 (s, NH), 7.75 (d, CHAr, J = 1.8 Hz), 7.44 (dd, CH Ar, J = 2.8 Hz), 7.38 (d, CHAr, J = 7.8 Hz), 6.84 (s, CHAr, J = 4.8 Hz), 3.52 (s, OCH_3), 2.76–2.74 (m, 2H, CH_2cyclo, C6), 2.56–2.53 (m, 2H, CH_2cyclo, C5); ^{13}C NMR ($CDCl_3$) δ: 167.28 (pyridine C), 165.22 (C═O), 143.04, 142.27, 128.48 (Ar-C), 118.20 (CN), 29.45 (C-5), 27.45 (C-6); Anal. calc. for $C_{19}H_{14}N_2O_3$: C, 71.69, H, 4.43, N, 8.80; Found: C, 71.65, H, 4.38, N, 8.76; ESI-MS m/z (rel. int. %): 320 (63) $[M + H]^+$

3.3.5. 4-(1,3-benzodioxol-5-yl)-8-methoxy-2-oxo-1,2,5,6-tetrahydrobenzo [h]quinoline-3-carbonitrile (QD5)

Yield: 78.34 (%); M.P: 218 °C; FTIR (KBr) ν_{max} cm^{-1}: 3233 (NH), 2927 (C−H), 2217 (CN), 1605 (C═O), 1562 (C═C), 1234 (N═C); ^{1}H NMR (600 MHz $CDCl_3$) (δ/ppm): 8.11 (s, NH), 7.71–6.79 (m, 6H, CHAr), 3.72 (s, OCH_3), 2.72–2.74 (m, 2H, CH_2cyclo, C6), 2.53–2.50 (m, 2H, CH_2cyclo, C5);); ^{13}C NMR ($CDCl_3$) (δ/ppm): 165.56 (pyridine C), 163.01 (C═O), 154.39, 152.23, 148.69, 129.74, 125.28 (Ar-C), 116.01 (CN), 28.56 (C-5), 26.98 (C-6); 143.04, 142.27, 128.48 (Ar-C), 118.20 (CN), 29.45 (C-5), 27.45 (C-6); Anal. calc. for $C_{22}H_{16}N2O_4$: C, 70.96, H, 4.33, N, 7.52; Found: C, 70.92, H, 4.28, N, 7.48; ESI-MS m/z (rel. int. %): 374 (85) $[M+H]^+$

3.4. DFT studies

All the five molecules QD**1**-QD5, were optimized using Spartan'08 Windows graphical software using Density Functional Theory (DFT) calculations with RB3LYP method [34]. The RB3LYP is the restricted version of B3LYP exchange-correlation functional [35]. This method has been previously used successfully for the calculation of small molecules [36]. Nevertheless, the structure were modeled and optimized using semiempirical PM3 method followed by the Hartree-Fock model with 6-31G* basis set. The obtained resulting wavefunction, Hessian matrix and geometry calculated were subjected for the final DFT

calculation with 6-31G* basis set. The asterisk means that the "d" polarization functions were added for Carbon and Oxygen atoms. The fundamental frequencies of all studied structures were also calculated and assigned as minima (all real frequencies).

3.5. Docking studies

The ligands (**QD1-QD4**) were drawn in ChemDraw Ultra 6.0 (Chem Office package) assigned with proper 2D orientation and analyzed for connection error in bond order. Dundee PRODRG2 server was used to minimize the energy of the molecules [37,38]. The energy minimized compounds were then read as input for AutoDock 4.2, in order to carry out the docking simulation. Crystal structure of DNA gyrase was obtained from Protein Data Bank (http://www.pdb.org/ pdb/home/home.do) with the PDB ID 1KZN. Auto Dock used the local search to search for the optimum binding site of small molecules to the protein. The active site was defined by a grid box of 85 × 80 × 90 points and spacing of 0.375 Å with the ligand binding site as the center. The final structure was then saved in pdbqt format. During the docking process, a maximum of 10 conformers were considered for each compound. All the AutoDock docking runs were performed on Intel Core2Duo CPU, with 4 GB DDR2 RAM. AutoDock 4.2 and AutoDock vina was compiled and run under Windows 7 operating system [28].

3.6. Antimicrobial susceptibility tests

3.6.1. Strains and media

Two Gram-positive bacteria (*Staphylococcus aureus* ATCC 29213 and *Streptococcus pyogenes* ATCC 19615) and two Gram-negative bacteria (*Escherichia coli* ATCC 25922 and *Salmonella typhimurium* ATCC14028) were used in this study. All microorganisms were sub-cultured in nutrient medium (beef extract 3 g/L; peptone 5 g/L; pH 7.0) and incubated for 24 h at 37 °C.

3.6.2. Disc diffusion assay:

To determine the antibacterial activity of the newly synthesized compounds, disc diffusion assay was employed. The assay was done as described previously with minor modifications [39].

Briefly, all the bacterial strains were grown in BHI medium for 24 h at 37 °C. After incubation, cells were spun down and approximately 10^5 CFU/mL were inoculated in a molten sterile nutrient agar at down 40 °C and poured onto an agar plate in a laminar flow cabinet. Five sterile paper discs (6.0 mm diameter) impregnated with 10, 20, 25, 50, and 100 μg/mL of test compounds prepared in 1% DMSO were fixed onto nutrient agar plate. Ciprofloxacin (10 μg/mL/disc) was used as standard drug (positive control) and DMSO (1%) poured disc was used as negative control. The susceptibility of the bacteria to the test compounds was determined by the formation of an inhibitory zone measured in mm, after 24 h of incubation at 37 °C.

3.6.3. Determination of minimal inhibitory concentration

Minimum inhibitory concentration (MIC) of the test compounds were evaluated by following Clinical and Laboratory Standards Institute (CLSI) recommended macro-broth dilution method M07-A9 and M07-A10 (CLSI. Methods for dilution antimicrobial susceptibility tests for bacteria Vol. 32 No. 2, 2012 and Vol. 35, No. 2, 2015). Test compounds (1 mL), previously dissolved in 1% DMSO, was added to the test tube containing 1 mL of broth media and serial dilutions were done to obtain the final concentrations of 512, 256, 128, 64, 32, 16, 8, 4, 2 and 1 μg/mL. Following serial dilutions, 1 mL of bacterial cultures, following standard inoculum of 10^5 CFU/ml, was added to each tube. The MIC, defined as the lowest concentration of the test compound, which inhibits the visible growth after 24 h, was determined visually after incubation for 24 h at 37 °C. Tests using 1% DMSO and ciprofloxacin were also included as negative and positive controls respectively.

3.7. Cytotoxicity studies (MTT assay)

3.7.1. Cell culture

Epithelial, human breast cancer cell line (MDA-MB-231) was cultured in Dulbecco's modified Eagle's medium with 10% fetal bovine serum (heat inactivated), 100 units mL^{-1} penicillin, 100 μg mL^{-1} streptomycin, and 2.5 μg mL^{-1} amphotericin B, at 37 °C in a saturated humidity atmosphere containing 95% air/5% CO_2 [40]. The cell lines were harvested when they reached 80% confluence to maintain exponential growth.

3.7.2. MTT assay

The MTT assay is a standard colorimetric assay, in which mitochondrial activity is measured by splitting tetrazolium salts with mitochondrial dehydrogenases in viable cells only [23]. For viability testing, MTT (3-(4,5-dimethylthiazole-2-yl)-2,5-diphenyl tetrazolium bromide, M2128 from Sigma) cell proliferation assay was carried out. The cell monolayers in exponential growth were harvested using 0.25% trypsin and single-cell suspensions were obtained by repeated pipetting. Only viable cells were used in the assay. Exponentially growing cells were plated at 1.2×10^4 cells per well into 96-well plates (Costar, Corning, NY, USA) and incubated for 48 hr before the addition of drugs to achieve the maximum confluency of the cells. Stock solutions were prepared by dissolving the compounds in 1% (v/v) DMSO and further diluted with fresh complete medium to achieve 1 mM/mL concentration. Cells were incubated with different concentrations of ciprofloxacin and test compounds for 48 h at 37 °C in 5% CO_2 humidified incubator together with untreated control sample. At appropriate time points, cells were washed in PBS, treated with 50 μL MTT solution (5 $mgmL^{-1}$, tetrazolium salt) and incubated for 4 h at 37 °C. At the end of the incubation period, the medium was removed and pure DMSO 150 μL was added to each well. The metabolized MTT product dissolved in DMSO was quantified by measuring the absorbance at 570 nm on an Microplate reader (iMark, BIORAD, S/N 10321) with a reference wavelength of 655 nm. All assays were performed in triplicate and repeated thrice. Percent viability was defined as the relative absorbance of treated versus untreated control cells.

4. Conclusions

One pot synthesis of Quinoline 3-carbonitrile derivatives by the reaction of appropriate aldehydes, 6-methoxy-1,2,3,4-tetrahydronaphthalin-1-one, ethyl cyanoacetate and ammonium acetate was achieved. All the compounds share a common basic ring skeleton except the presence of different aryl substituents at position-4 of the quinoline ring. The presence of furan ring in compound QD**4** seems to have a prominent effect on the biological profile of the molecule compared to the other analogues. It seems that the presence of a heteroaromatic ring with lone pair of electrons at position-4 of the quinoline nucleus helps the compound to achieve better antibacterial activity, possibly due to stronger interactions or more binding affinity with the target. However, the structure further needs to be optimized with different heteroaromatic rings or electron withdrawing or electron releasing substituted rings to further verify these preliminary results. The comparatively softer nature of compound QD**4**, lower band gap energy of 3.40 eV and a low-lying LUMO helps the molecule to achieve higher antibacterial activity possibly due to better interaction with the target compared to the other structurally related derivatives. All the derivatives, however, obeyed the Lipinski's rule of 5 and possessed desirable physico-chemical properties. To gain better understanding of structure–activity relationship and to get the most optimal molecule we are currently optimising the structure of these molecules by replacing the furan ring with other heteroaromatic moieties which will be reported in due course of time.

Acknowledgments

The authors are thankful to the Chemistry Department at King Abdulaziz University for providing research facilities.

Declaration of Competing Interest

None to declare.

Appendix A. Supplementary material

Supplementary data to this article can be found online at https://doi.org/10.1016/j.bioorg.2019.102968.

References

[1] R.S. Keri, S.A. Patil, Biomed. Pharmacother. 68 (2014) 1161–1175.
[2] N.C. Desai, K.M. Rajpara, V.V. Joshi, Bioorg. Med. Chem. Lett. 22 (2012) 6871–6875.
[3] N. Ahmed, K.G. Brahmbhatt, S. Sabde, D. Mitra, I.P. Singh, K.K. Bhutani, Bioorg. Med. Chem. 18 (2010) 2872–2879.
[4] M.I. Abdullah, A. Mahmood, M. Madni, S. Masood, M. Kashif, Bioorg. Chem. Biomed. Pharmacother. 54 (2014) 31–37.
[5] C. Theeraladanon, M. Arisawa, A. Nishida, M. Nakagawa, Tetrahedron 60 (2004) 3017–3035.
[6] K.M. El-Gamal, A.M. El-Morsy, A.M. Saad, I.H. Eissa, M. Alswah, J. Mol. Str. 1166 (2018) 15–33.
[7] M.E. Zayed, P. Kumar, J. Fluorescen. 27 (2017) 853–860.
[8] S.A. Khan, J. Fluorescen. 27 (2017) 929–937.
[9] G.S. Bisacchi, J. Med. Chem. 58 (2015) 4874–4882.
[10] M.J. Mitton-Fry, S.J. Brickner, J.C. Hamel, L. Brennan, J.M. Casavant, M. Chen, T. Chen, X. Ding, J. Driscoll, J. Hardink, T. Hoang, E. Hua, M.D. Huband, M. Maloney, A. Marfat, S.P. McCurdy, D. McLeod, M. Plotkin, U. Reilly, S. Robinson, J. Schafer, R.M. Shepard, J.F. Smith, G.G. Stone, C. Subramanyam, K. Yoon, W. Yuan, R.P. Zaniewski, C. Zook, Bioorg. Med. Chem. Lett. 23 (2013) 2955–2961.
[11] Frédéric Collin, Shantanu Karkare, Anthony Maxwell, Appl. Microbiol. Biotechnol. 92 (2011) 479–497.
[12] Anthony Maxwell, Trends Microbiol. 5 (1997) 102–108.
[13] K.M. Evans-Roberts, L.A. Mitchenall, M.K. Wall, J. Leroux, J.S. Mylne§, A. Maxwell, J. Biolog. Chem. 291 (2016) 3136–3144.
[14] J.-M. Rolain, C. Abat, M.-T. Jimeno, P.-E. Fournier, D. Raoult, Clin. Microbiol. Inf. 22 (2016) 408–415.
[15] Miki Akamatsu, J. Agric. Food Chem. 5 (2011) 2909–2917.
[16] J.A. Arnott, S.L. Planey, Expert Opin. Drug Discov. 7 (2012) 863–875.
[17] J.A. Arnott, R. Kumar, S.L. Planey, J. App Biopharm. Pharcokin. 1 (2013) 31–36.
[18] N.A. Meanwell, Chem. Res. Toxicol. 24 (2011) 1420–1456.
[19] M.J. Waring, Expert Opin. Drug Discov. 5 (2010) 235–248.
[20] C.A. Lipinski, F. Lombardo, B.W. Dominy, P.J. Feeney, Adv. Drug Del. Rev. 46 (2001) 3–26.
[21] W. Curatolo Pharm, Sci. Technol. Today 19 (1998) 387–393.
[22] E.H. Kearns, L. Di, Drug-like Properties: Concepts, Structure Design and Methods, Elsevier, USA, 2008.
[23] M.P. Gleeson, J. Med. Chem. 51 (2008) 817–834.
[24] R.G. Pearson, J. Songstad, J. Am. Chem. Soc. 89 (1967) 1827–1836.
[25] G. Gece, Corros. Sci. 50 (2008) 2981–2992.
[26] S.B. Gopalakrishnan, T. Kalaiarasi, R. Subramanian, Linn. J. Comput. Meth. Phy. (2014) 6–12 ID 623235.
[27] K.D. Sen, D.M.P. Mingos, Chemical Hardness: Structure and Bonding, Springer, Berlin, Germany, 1993.
[28] O. Trott, A.J. Olson, J. Comput. Chem. 31 (2010) 455–461.
[29] H. Garn, H. Krause, V. Enzmann, K. Drossler, Immunol. Method 168 (1994) 253–256.
[30] M.Y. Wani, A.R. Bhat, A. Azam, I. Choi, F. Athar, Eur. J. Med. Chem. 48 (2012) 313–320.
[31] World Health Organization, Global Priority List of Antibiotic-Resistant Bacteria to Guide Research, Discovery, and Development of New Antibiotics, 2017. < http://www.who.int/medicines/publications/global-priority-list-antibi otic-resistant-bacteria/en/ > .
[32] N. Jackson, L. Czaplewski, L.J.V. Piddock, J. Antimicrob. Chemother. 1 (2018) 1452–1459.
[33] E. Lippert, Z. Electrochem. 61 (1957) 962–975.
[34] Spartan'08 Version 1.2.0, Wavefunction, Inc., 18401 Von Karman Ave., Suite 370, Irvine, CA 92612, USA.
[35] S.A. Khan, A.M. Asiri, K. Sharma, Med. Chem. Res. 22 (2013) (2004) 1998.
[36] S. Kumarn, V.C. Rao, R.C. Rastogi, Spectrochim. Acta A 57 (2001) 41–47.
[37] S. Mouilleron, M.A. Badet-Denisot, B. Golinelli-Pimpaneau, J. Mol. Biol. 377 (2008) 1174, https://doi.org/10.1016/j.jmb.2008.01.077.
[38] T. Sander, J. Freyss, M. von Korff, J.R. Reich, C. Rufener, J. Chem. Inf. Model 49 (2009) 232–246.
[39] A. Ahmad, A. Khan, N. Manzoor, L.A. Khan, Microb. Pathogen. 48 (2010) 35–41.
[40] M.M.C. Ferrari, A.M. Fornasiero, M.T.T. Isetta, J. Immunol. Meth. 131 (1990) 165–172.